

Topological Winding and Unwinding in Metastable Bose-Einstein Condensates

Rina Kanamoto,¹ Lincoln D. Carr,² and Masahito Ueda^{3,4}

¹Department of Physics, University of Arizona, Tucson, Arizona, 85721, USA

²Department of Physics, Colorado School of Mines, Golden, Colorado, 80401, USA

³Department of Physics, Tokyo Institute of Technology, Meguro-ku, Tokyo 152-8551, Japan

⁴ERATO, JST, Bunkyo-ku, Tokyo 113-8656, Japan

(Received 24 April 2007; published 12 February 2008)

Topological winding and unwinding in a quasi-one-dimensional metastable Bose-Einstein condensate are shown to be manipulated by changing the strength of interaction or the frequency of rotation. Exact diagonalization analysis reveals that quasidegenerate states emerge spontaneously near the transition point, allowing a smooth crossover between topologically distinct states. On a mean-field level, the transition is accompanied by formation of gray solitons, or density notches, which serve as an experimental signature of this phenomenon.

DOI: 10.1103/PhysRevLett.100.060401

PACS numbers: 03.75.Hh, 03.75.Lm

Metastability of a physical system leads to a rich variety of quantum phases and transport properties that are not present in the ground-state phase. An illustrative example is superflow and phase slip in a narrow superconducting channel [1]. Other examples include Feshbach molecules formed in high rotational states [2] and metastable quantum phases in higher Bloch bands in an optical lattice [3]. Recent experimental advances in cold atoms or molecules have made it possible to realize excited, metastable states which persist for a long time. These states provide an excellent medium in which to investigate fundamental aspects of condensed matter systems such as topological excitations and superfluidity [4–7].

It is widely believed that the angular momentum per particle in a weakly repulsive one-dimensional (1D) superfluid ring system [6,7] is quantized at $T = 0$ and that there are discontinuous jumps between states having different values of the phase winding number. In this Letter, we point out that this applies only to the ground state; continuous transitions do in fact occur between metastable states of repulsive condensates. The underlying physics behind this phenomenon is the emergence of a dark or gray soliton train [8] which bifurcates from the plane-wave solution and carries a fraction of the quantized value of the angular momentum.

Starting with mean-field theory for scalar bosons subject to rotation, we proceed through progressively deeper levels of insight into the quantum many-body nature of this problem, making a link between semiclassical and quantum solitons in metastable states. We find that the phase slip, which allows a smooth crossover between topologically distinct states, is caused by a *quantum soliton*. The latter consists of a linear superposition of the rotationally-invariant many-body eigenstates of the Hamiltonian [9]. In both Bogoliubov theory and quantum many-body theory the broken-symmetry soliton state is shown to be stable against perturbation.

This phenomenon can be realized by hot atoms confined in fast-rotating circular waveguides or toroidal traps [10].

First, to obtain a metastable uniform condensate one quickly stops the rotation and then lowers the temperature. Second, one adiabatically changes the angular frequency of the trap in the presence of a small arbitrary perturbation in the trapping potential. This causes atoms to adiabatically take the higher-energy path of a metastable soliton state, as we will show. Third, one stops the adiabatic change in the frequency at the correct point to arrive at a different winding number. All of these processes can occur continuously.

We consider a system of N bosonic atoms in a quasi-1D torus with radius R , under an external rotating drive with angular frequency 2Ω . The length, angular momentum, and energy are measured in units of R , \hbar , and $\hbar^2/(2mR^2)$, respectively. The Hamiltonian is given by the Lieb-Liniger Hamiltonian in a rotating frame of reference [11,12],

$$\hat{H} = \int_0^{2\pi} d\theta [\hat{\psi}^\dagger (-i\partial_\theta - \Omega)^2 \hat{\psi} + g_{1D} \hat{\psi}^\dagger \hat{\psi}^2 / 2], \quad (1)$$

where g_{1D} characterizes the strength of the s -wave interatomic collisions in one dimension [13] rescaled by $\hbar^2/(2mR)$, θ is the azimuthal angle, and the bosonic field operator satisfies periodic boundary conditions: $\hat{\psi}(\theta) = \hat{\psi}(\theta + 2\pi)$. Since the Hamiltonian is periodic with respect to Ω , the properties of the system are periodic in Ω with period 1 [14], in direct analogy to the reduced Brillouin zone in a Bloch band [7,15]. Without loss of generality we will henceforth restrict ourselves to $\Omega \in [0, 1)$. The Hamiltonian is integrable via the boson-fermion mapping in the Tonks-Girardeau (TG) limit $g_{1D} \gg N$ [16], and via the Bethe ansatz in the weak-interaction limit $g_{1D}N \lesssim O(1)$ as well as intermediate-interaction regimes.

We first show how continuous changes in the angular momentum occur in the weak-interaction regime for solutions of the Gross-Pitaevskii equation (GPE) $[(-i\partial_\theta - \Omega)^2 + g_{1D}N|\psi(\theta)|^2]\psi(\theta) = \mu\psi(\theta)$, where ψ is the order parameter normalized to unity and $\varphi \equiv \text{Arg}(\psi)$ is its phase. The single valuedness of the wave function requires $\varphi(\theta + 2\pi) = \varphi(\theta) + 2\pi J$, where $J \in \{0, \pm 1, \pm 2, \dots\}$ is

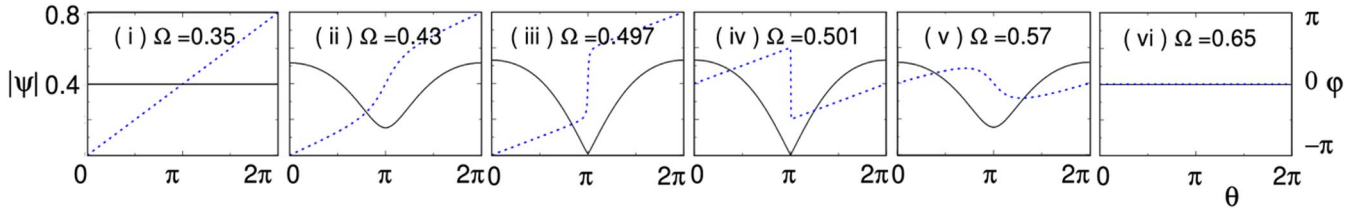


FIG. 1 (color online). Amplitude (solid curves with the left reference), and phase (dotted curves with the right reference) of metastable states of the GPE for $g_{1D}N = 0.6\pi$. Uniform solutions with different values of the phase winding (i) $J = 1$, and (vi) $J = 0$ are smoothly connected through the broken-symmetry gray soliton (ii)–(v) with a self-induced phase slip at $\Omega = 0.5$.

the topological winding number. Stationary solutions of the GPE for $g_{1D} \geq 0$ are either plane-wave states $\psi(\theta) = e^{ij\theta}/\sqrt{2\pi}$ or a gray soliton train [8] whose amplitude and phase are given by $|\psi(\theta)| = A[1 + \eta \text{dn}^2(jK(\theta - \theta_0)/\pi, k)]^{1/2}$, and $\varphi(\theta) = \Omega\theta + B\Pi(\xi; jK(\theta - \theta_0)/\pi, k)$, respectively. Here the amplitude $A \equiv \sqrt{K/[2\pi(K + \eta E)]}$; the phase prefactor $B \equiv (S/jK) \times \sqrt{g_{\text{sn}}h_{\text{sn}}/2f_{\text{sn}}}$; there are j density notches in the soliton train; $\eta = -2j^2K^2/g_{\text{sn}} \in [-1, 0]$ characterizes the depth of each density notch; $k \in [0, 1]$ is the elliptic modulus; $K(k)$, $E(k)$, $\Pi(\xi, u, k)$, are elliptic integrals of the first, second, and third kinds; and $\text{dn}(u, k)$ is the Jacobi dn function. The degeneracy parameter θ_0 indicates that the soliton solutions are broken-symmetry states. We define $f_{\text{sn}} = \pi g_{1D}N/2 - 2j^2K^2 + 2j^2KE$, $g_{\text{sn}} = f_{\text{sn}} + 2j^2K^2$, $h_{\text{sn}} = f_{\text{sn}} + 2k^2j^2K^2$, and $S = 1$ for $0 \leq \Omega < 0.5$, $S = -1$ for $0.5 \leq \Omega < 1$. Then $\xi = -2(kjK)^2/f_{\text{sn}} \leq 0$, and only when soliton solutions exist [17] is $k \neq 0$. In the limit $\eta \rightarrow -1$, f_{sn} approaches zero, and g_{sn} and h_{sn} both approach finite positive values; consequently, the wave function approaches the Jacobi sn function, which corresponds to a dark soliton with a π -phase jump at θ_0 . In the opposite limit $\eta \rightarrow 0$, both the amplitude and phase approach those of the plane-wave solution with the same phase winding J . These limiting behaviors indicate that continuous change in topology of the condensate wave function is possible, as illustrated in Fig. 1 (i)–(vi). Henceforth, we consider the single soliton $j = 1$ for simplicity, but our discussion holds for arbitrary soliton trains $j > 1$.

Bifurcation of the soliton train from the plane wave constitutes a second-order quantum phase transition with respect to g_{1D} and/or Ω . Figure 2(a) shows the energy difference $E_J^{(\text{sol})} - E_J^{(\text{pw})}$ between the two solutions

$$\begin{aligned} E_J^{(\text{pw})} &= (\Omega - J)^2 + g_{1D}N/(4\pi), \\ E_J^{(\text{sol})} &= g_{1D}N/(2\pi) + [3KE - K^2(2 - k^2)]/\pi^2 \\ &\quad + 4K^2[3E^2 - 2(2 - k^2)KE \\ &\quad + K^2(1 - k^2)]/(3\pi^3 g_{1D}N). \end{aligned}$$

This kind of bifurcation does not occur from the ground-state energy. However, for metastable states a bifurcation can occur between the plane-wave state and the soliton

state with the same winding number J . After bifurcation, the soliton energy $E_J^{(\text{sol})}$ becomes larger than $E_J^{(\text{pw})}$. Furthermore, at $\Omega = 0.5$, $E_0^{(\text{sol})}$ and $E_1^{(\text{sol})}$ are degenerate with a $\pm\pi$ -phase jump in the condensate wave function. The derivatives of the energies $\partial E_J^{(\text{sol})}/\partial\Omega$ and $\partial E_J^{(\text{pw})}/\partial\Omega$ have a kink at the boundary as can be verified analytically. This identifies the second-order quantum phase transition [18], which occurs along a curve in the Ω - g_{1D} plane.

Figures 1 (i)–(vi) illustrate a continuous change in the topology along a higher-energy, soliton path shown in Fig. 2(a) with white arrows. Following this path in Fig. 1, as Ω increases starting from (i) the plane wave with $J = 1$, (ii) solitons start to form past a critical point Ω_{cr} . (iii) The density notch deepens for $\Omega_{\text{cr}} \leq \Omega \leq 0.5$. At $\Omega = 0.5$ it forms a node, the phase of the soliton jumps by π , and the energies of the solitons with phase winding number 1 and 0 are degenerate. (iv),(v) The soliton with phase winding $J = 0$ deforms continuously as Ω increases. (vi) Finally, the state goes back to the plane-wave state with phase winding $J = 0$ [19].

The angular momentum $L/N = \int d\theta \psi^*(-i\partial_\theta)\psi$ of the metastable states changes continuously along the soliton path. For the plane-wave state, $L_J^{(\text{pw})}/N = J$ is quantized; in contrast, for the soliton $L_J^{(\text{sol})}/N = \Omega + \mathcal{S}\sqrt{2f_{\text{sn}}g_{\text{sn}}h_{\text{sn}}}/(g_{1D}N\pi^2)$ is noninteger, as shown in Fig. 2(b). Thus a continuous change of angular momentum is possible for 1D Bose systems by taking the metastable states with energy slightly higher than that of the ground state.

We next investigate the stability of the metastable states using Bogoliubov theory [20,21], and identify the curve in the Ω - g_{1D} plane where the soliton solutions bifurcate from the plane-wave solutions. A stationary solution ψ of the GPE subject to a small perturbation δ evolves in time as $\tilde{\psi}(t) = e^{-i\mu t}[\psi + \sum_n(\delta u_n e^{-i\lambda_n t} + \delta v_n^* e^{i\lambda_n^* t})]$, where (u_n, v_n) and λ_n are eigenstates and eigenvalues of the Bogoliubov–de Gennes equations (BdGE), and n denotes the index of the eigenvalues.

For the plane-wave state with phase winding J , the eigenvalues of the BdGE are obtained as $\lambda_n^{(J, \text{pw})} = [n^2(n^2 + g_{1D}N/\pi)]^{1/2} - 2n(\Omega - J)$. Then $\lambda_{-1}^{(J=1, \text{pw})}$ is negative, monotonically increases for $\Omega \in [0, \Omega_{\text{cr}}]$, and crosses zero at $(g_{1D}N)_{\text{cr}}/(2\pi) - 2(\Omega_{\text{cr}} - J)^2 + 1/2 = 0$.

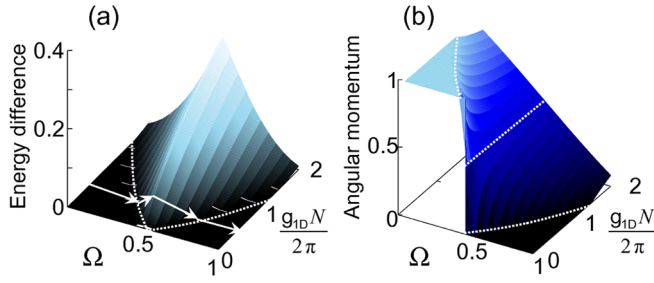


FIG. 2 (color online). (a) Energy difference between the metastable plane-wave and soliton states. The soliton solutions exist in the area surrounded by two phase boundaries (white dotted curves). (b) Corresponding angular momentum. The soliton solutions make it possible to smoothly connect quantized integer values of average angular momentum.

Thus the metastable state $\psi = e^{i\theta}/\sqrt{2\pi}$ is *thermodynamically* unstable. The plane-wave limit of the soliton solutions $\eta \rightarrow 0$ occurs when $(g_{1D}N, \Omega)$ approach their critical values from above. We also obtained the eigenvalues of the BdGE when ψ is taken as a soliton. The eigenstates obtained from a soliton involve the Nambu-Goldstone mode $\lambda_{\text{NG}}^{(J=1,\text{sol})}$, i.e., the zero-energy rotation mode, associated with the rotational symmetry breaking of the soliton solution. At the critical values of $(g_{1D}N, \Omega)$, $\lambda_{-1}^{(J=1,\text{pw})} = \lambda_{\text{NG}}^{(J=1,\text{sol})}$ and other eigenvalues $\lambda^{(J,\text{sol})}$ are nearly degenerate with $\lambda^{(J,\text{pw})}$. There is no negative Bogoliubov mode in the soliton regime. Thus the soliton state is linearly stable.

Finally, we investigate how continuous change in the angular momentum per particle observed in the mean-field theory is described in terms of quantum many-body theory. Lieb derived two kinds of excitation branches in the thermodynamic limit, “type I” and “type II” excitation branches of Eq. (1) with $\Omega = 0$ [11]. The type II excitation was shown to be a dark soliton branch [22]. We also determined low-lying excitation energies in a finite-size waveguide in a wide range of $g_{1D}N$ via the Bethe ansatz [23–25].

In order to study the metastable states we need to investigate the N th order highly excited states. We diagonalize Eq. (1) in a basis which provides equivalent results to those obtained with the Bethe ansatz [26] for the purposes of physical insight. The basis is taken as $|n_{-1}, n_0, n_1, n_2\rangle$, subject to conditions $\sum_l n_l = N$ and $\sum_l l n_l = L$, where n_l is the number of atoms with single-particle angular momentum l and $L \in \{-N, \dots, 2N\}$ is the total angular momentum. Figure 3(a) shows the energies $E_L \equiv \langle L, N | \hat{H} | L, N \rangle$ of yrast states $|L, N\rangle$, i.e., the lowest-energy state for a fixed value of L and N . The index N will be dropped, as it is fixed. The curvature of the surface is independent of N but the density of states with respect to L/N increases as N becomes larger. Three kinds of states appear in this energy landscape: (i) Ground state: The ground state of the Hamiltonian is $|L=0\rangle$ with energy $E_{L=0}/N \simeq \Omega^2 + g_{1D}N/(4\pi)$ for $\Omega \in [0, 0.5)$, and $|L=N\rangle$ with en-

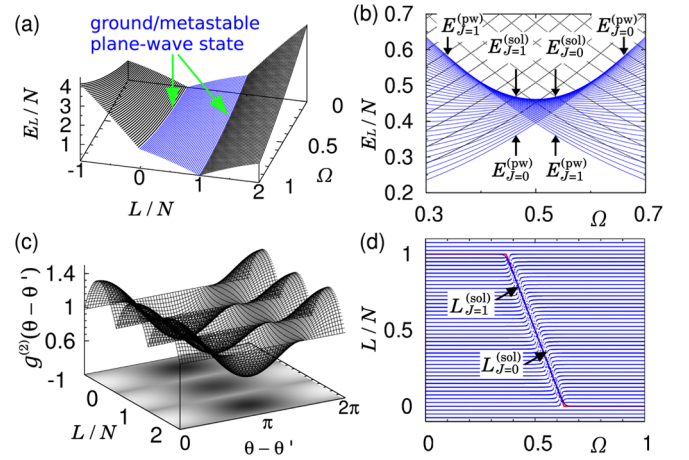


FIG. 3 (color online). (a) The lowest energy of the Hamiltonian for each angular-momentum subspace for $N = 40$, $g_{1D} = 2\pi \times 7.5 \times 10^{-3}$. (b) Enlargement of (a) near the critical point. Densely packed blue curves are spectra within $L \in \{0, N\}$. Otherwise the spectra are sparse. (c) Two-body correlation function of eigenstates for each angular-momentum subspace. (d) Expectation value of the angular momentum of each eigenstate, in the presence of symmetry-breaking potential \hat{V} as a function of Ω .

ergy $E_{L=N}/N \simeq (\Omega - 1)^2 + g_{1D}N/(4\pi)$ for $\Omega \in [0.5, 1)$, respectively. These are in agreement with the mean-field ground states $\psi = 1/\sqrt{2\pi}$ and $\psi = e^{i\theta}/\sqrt{2\pi}$, respectively. (ii) Metastable plane-wave states: Similarly, the many-body counterparts of the metastable plane-wave solutions of the GP equation are $|L=N\rangle$ for $0 \leq \Omega < 0.5$ and $|L=0\rangle$ for $0.5 \leq \Omega < 1$, respectively. (iii) Seeds of broken-symmetry states: All many-body eigenstates are rotationally invariant because they respect the symmetry of the Hamiltonian; i.e., there are *no* broken-symmetry eigenstates. However, as shown in Fig. 3(b), the eigenvalues $\{E_{L=0}, \dots, E_N\}$ (densely packed blue curves) cross each other in between the ground and metastable plane-wave states, and $\{E_{L=1}, \dots, E_{N-1}\}$ become larger than the metastable plane-wave state energies within a certain range of Ω . The regime of this quasidegenerate level crossing can be identified with the soliton regime given by the mean-field theory, as we will show. Furthermore, the envelope of the highest eigenvalues in the quasidegenerate regime coincides with $E_{J=0,1}^{(\text{sol})}$ in the limit $N \rightarrow \infty$. In the absence of interaction ($g_{1D} = 0$), all the levels with $L \in \{0, N\}$ are degenerate for $\Omega = 0.5$ only. The degeneracy inherent in a level crossing permits the existence of a broken-symmetry state; in our case, this is the soliton solution corresponding to the mean-field theory prediction.

Figure 3(c) shows the two-body correlation function $g^{(2)}(\theta - \theta') \equiv \langle \hat{\psi}^\dagger(\theta)\hat{\psi}^\dagger(\theta')\hat{\psi}(\theta')\hat{\psi}(\theta) \rangle / [\langle \hat{\psi}^\dagger(\theta)\hat{\psi}(\theta) \rangle \times \langle \hat{\psi}^\dagger(\theta')\hat{\psi}(\theta') \rangle]$, where the expectation value is taken with respect to each yrast state $|L\rangle$. The function $g^{(2)}$ is independent of Ω and has a single peak. When L/N is an

integer, $g^{(2)} = 1$; when L/N is half-integer, $g^{(2)}$ strongly deviates from 1. The one-body density $g^{(1)} \equiv \langle \hat{\psi}^\dagger(\theta)\hat{\psi}(\theta) \rangle = 2\pi/N$ is a constant for any eigenstate, since the system is rotationally invariant.

In order to force *quantum solitons* to appear in $g^{(1)}$, we add a symmetry-breaking perturbation of the form $\hat{V} = \varepsilon \sum_{l \in \{-1, 0, 1, 2\}} (\hat{c}_{l+1}^\dagger \hat{c}_l + \text{h.c.})$, $\varepsilon \ll g_{1D}$. The total angular momentum L is no longer a good quantum number, and the eigenvalue problem is thus given in a general form, $(\hat{H} + \hat{V})|\Psi_n\rangle = E_n|\Psi_n\rangle$ where $n \in \{0, 1, \dots\}$ is the energy eigenvalue index. Employing the basis $|L\rangle$, where $L \in \{-N, 2N\}$, the average angular momentum per particle is shown in Fig. 3(d) for each eigenstate for $\varepsilon = 5 \times 10^{-3}$. Outside the soliton regime, angular momenta remain integer values unaffected by the small perturbation. In the soliton regime, on the other hand, by a superposition of eigenstates $|L\rangle$ in the absence of the perturbation some of the angular momenta converge to a noninteger value, which indeed agrees with $L_{j=0,1}^{(\text{sol})}$. We have also calculated the one-body correlation function $g^{(1)}$ for all eigenstates in the presence of the symmetry-breaking perturbation, and confirm that $g^{(1)}$ has a single density notch in the soliton regime with the depth close to the mean-field gray soliton.

In conclusion, we found a denumerably infinite set of paths to connect plane-wave states via soliton trains in a metastable system of scalar bosons on a ring. Associated with this transition, the energy of the solitons bifurcates, and a continuous change in the angular momentum becomes possible in the mean-field theory. We made a link between these mean-field results and the full quantum theory by showing that quasidegenerate energy levels are related to the formation of quantum solitons.

We thank Joachim Brand and Yvan Castin for useful discussions. This material is based upon work supported by the National Science Foundation under Grant No. PHY-0547845 as part of the NSF-CAREER program, and a Grant-in-Aid for Scientific Research (Grant No. 17071005).

-
- [1] J.S. Langer and V. Ambegaokar, Phys. Rev. **164**, 498 (1967).
 [2] S. Knoop *et al.*, arXiv:0710.4052.
 [3] V.W. Scarola and S. Das Sarma, Phys. Rev. Lett. **95**, 033003 (2005).
 [4] V. Schweikhard *et al.*, Phys. Rev. Lett. **93**, 210403 (2004); A. E. Leanhardt *et al.*, Phys. Rev. Lett. **90**, 140403 (2003); M. Nakahara *et al.*, Physica (Amsterdam) **284B**, 17 (2000); T. Isoshima *et al.*, Phys. Rev. A **61**, 063610 (2000).

- [5] A.J. Leggett, Rev. Mod. Phys. **71**, S318 (1999).
 [6] N. Byers and C.N. Yang, Phys. Rev. Lett. **7**, 46 (1961); S.J. Putterman, M. Kac, and G.E. Uhlenbeck, Phys. Rev. Lett. **29**, 546 (1972).
 [7] F. Bloch, Phys. Rev. A **7**, 2187 (1973).
 [8] L.D. Carr, C.W. Clark, and W.P. Reinhardt, Phys. Rev. A **62**, 063611 (2000).
 [9] R. Kanamoto, H. Saito, and M. Ueda, Phys. Rev. Lett. **94**, 090404 (2005).
 [10] S. Gupta *et al.*, Phys. Rev. Lett. **95**, 143201 (2005); A.S. Arnold, C.S. Garvie, and E. Riis, Phys. Rev. A **73**, 041606(R) (2006); S.R. Muniz *et al.*, Opt. Express **14**, 8947 (2006); C. Ryu *et al.*, Phys. Rev. Lett. **99**, 260401 (2007).
 [11] E.H. Lieb and W. Liniger, Phys. Rev. **130**, 1605 (1963); E.H. Lieb, Phys. Rev. **130**, 1616 (1963).
 [12] The Hamiltonian includes a constant term proportional to Ω^2 which is associated with rigid-body rotation and only shifts the origin of the total energy. The many-body wave functions $\Psi_{\text{rot}}(\{\theta\})$ of this Hamiltonian are obtained by the transformation of the solution $\Psi_{\text{lab}}(\{\theta\})$ in the rest frame (original Lieb-Liniger Hamiltonian), via $\Psi_{\text{rot}}(\{\theta\}) = \prod_j \exp(2i\Omega\theta_j)\Psi_{\text{lab}}(\{\theta\})$.
 [13] M. Olshanii, Phys. Rev. Lett. **81**, 938 (1998).
 [14] This periodicity in Ω is associated with the *umklapp* process of the total momentum $L' = L + JN$ as was pointed to in [11].
 [15] R. Bhat *et al.*, Phys. Rev. A **74**, 063606 (2006).
 [16] M. Girardeau, J. Math. Phys. (N.Y.) **1**, 516 (1960).
 [17] $2\pi\Omega S = 2(1 - k^2)(jK)^2 2f_{\text{sn}}/(g_{\text{sn}}h_{\text{sn}}) + \sqrt{2f_{\text{sn}}h_{\text{sn}}/g_{\text{sn}}} + j\pi[1 - \Lambda_0(\epsilon \setminus \alpha)]$, where Λ_0 is Heuman's lambda function, $\alpha = \arcsin k$, and $\epsilon \equiv \arcsin(f_{\text{sn}}/h_{\text{sn}})$.
 [18] S. Sachdev, *Quantum Phase Transitions* (Cambridge University Press, Cambridge, England, 1999).
 [19] We note that the amplitude remains uniform, and the phase looks like Fig. 1(i) for $\Omega \in [0, 0.5)$, and Fig. 1(vi) for $\Omega \in [0.5, 1)$ with a π -phase jump at $\Omega = 0.5$, if one takes the lower energy path.
 [20] A.L. Fetter and A.A. Svidzinsky, J. Phys. Condens. Matter **13**, R135 (2001).
 [21] L.J. Garay *et al.*, Phys. Rev. Lett. **85**, 4643 (2000).
 [22] M. Ishikawa and H. Takayama, J. Phys. Soc. Jpn. **49**, 1242 (1980).
 [23] J. Brand, J. Phys. B **37**, S287 (2004).
 [24] A.G. Sykes, P.D. Drummond, and M.J. Davis, Phys. Rev. A **76**, 063620 (2007).
 [25] The angular-momentum states $|L\rangle$ correspond to the different excited states of "Type I" in the finite-size Bethe-ansatz approach to the Lieb's Hamiltonian, where $L = \sum_j (k_j - \Omega)^2$ with $k_j (j = 1, \dots, N)$ being the quasi-momenta.
 [26] For our interaction regime the convergence of this truncation is confirmed by the comparison with the finite-size Bethe-ansatz method.